

Shape of Fractal Growth Patterns: Exactly Solvable Models and Stability Considerations

Itamar Procaccia and Reuven Zeitak

Department of Chemical Physics, The Weizmann Institute of Science, Rehovot 76100, Israel

(Received 1 February 1988)

Fractal, dendritic patterns with invariant distributions which are harmonic measures are represented by Julia sets of polynomial mappings. The equipotential lines around such patterns are obtained, leading to analytic estimates of the minimal and maximal scaling exponents of the $f(\alpha)$ function of the harmonic measure. These and physical stability arguments rationalize the shapes of diffusion-limited aggregates.

PACS numbers: 68.70.+w

Fractal growth patterns appear in a variety of related problems, like electrodeposition,¹ colloidal aggregation,² dielectric breakdown,³ and viscous fingering.⁴ A useful model for these phenomena is the Witten-Sander diffusion-limited aggregation (DLA) model.⁵ On the face of it, the DLA model seemed simple, and one could have hoped for a speedy solution at least in two dimensions. In fact, all attempts at rigorous solutions failed, repeatedly, and one is not sure what is the exact fractal dimension of DLA, and even whether there exists a limiting dimension for large aggregates.

A clue to the true complexity of the problem (which at the early stages was masked by the belief that the aggregates are fully characterized by their fractal dimension) was obtained from the discovery⁶ that the harmonic measure is a multifractal measure characterized by a spectrum of generalized dimensions. The harmonic measure is tantamount to the probability that a random walker would hit the boundary of the aggregate, and thus determines (in a yet unfathomed self-consistent way) its growth and its shape. By a multifractal measure one means⁷ that the measure of any ball of radius l scales like $P(l) \sim l^\alpha$, but with an α that takes on a range of values $\alpha_{\min} \leq \alpha \leq \alpha_{\max}$. How common a value of α is measured by the function $f(\alpha)$, which can be interpreted⁷ as the dimension of the subset that supports a scaling exponent α .

A surprisingly good prediction for the leading singularity (the minimal scaling exponent α_{\min}) is obtained from the "large wedge" model.^{6,8} Imagining stretching a rubber band around a DLA grown off lattice in two dimensions, one finds a rough pentagonal symmetry. Neglecting now the ramified structure, and calculating the singularity of an electric field at a wedge of included angle $\beta = 108^\circ$, one predicts a value for α_{\min} , $\alpha_{\min} = \frac{2}{7}$. For DLA grown on square lattices, a wedge of 90° leads to $\alpha_{\min} = \frac{2}{3}$. [In general, for m major fingers, one predicts^{6,8} $\alpha_{\min} = \pi/(2\pi - \beta) = m/(m+2)$.] A scaling argument^{6,8} leads to a prediction for the fractal dimension D_0 , $D_0 = 1 + \alpha_{\min}$, and the respective values $D_0 \approx 1.71$, $D_0 = 1.66$ for DLA grown off lattice and on a square lattice seem acceptable. Why a large-wedge model works

so well remained somewhat of a mystery.

On the other hand, the scaling at the fjords (the invaginated regions) is expected to contribute the largest scaling exponent α_{\max} . How this happens, and whether there is a relation between α_{\max} and the geometry, is completely unknown. Simulations fail to yield reliable information about this range of scaling exponents since the harmonic measure is so small in the fjords.

The aim of this Letter is to justify the large-wedge model. The reason that it is important is that once it is accepted, it leads, via physical stability arguments, to an estimate of the number of prominent branches that one expects in a DLA. The number of major tips in a DLA is determined by a competition between two effects. On the one hand, if there are too many equally long branches (the limit of circular symmetry) the Mullins-Sekerka instability⁹ sets in to distort the situation in favor of fewer major tips. On the other hand, if the number of major tips is too small, the fjords are too open, and minor branches can grow, increasing the number of major tips. It was shown by Ball¹⁰ that a balance can be obtained, and that *if one accepts the large-wedge model*, then the DLA should have an α_{\min} that satisfies the relation $\alpha_{\min}(\frac{1}{2}m - 1) = 1$, where m is the number of major fingers. Using $\alpha_{\min} = m/(m+2)$, we find $\alpha_{\min} \approx 0.707$ in good agreement with off-lattice DLA. It thus becomes crucial to gain a better understanding of why and when the large-wedge model is expected to work. To achieve it we introduce and solve a family of exactly solvable models which exhibit complex ramified fractal objects, with any desired number of major fingers, whose harmonic measures can be exactly calculated, and whose spectra of scaling exponents can be systematically obtained. We propose that these models can be used to understand some of the observed properties of growth patterns, that to us seem important. It is possible to calculate α_{\min} and α_{\max} , and to relate their value to the geometry. In particular these models allow us an exact calculation of the equipotential lines around the (charged) fractal, indicating why (and when) the large-wedge theory works. They also allow relating the scaling in the fjords to the geometry.

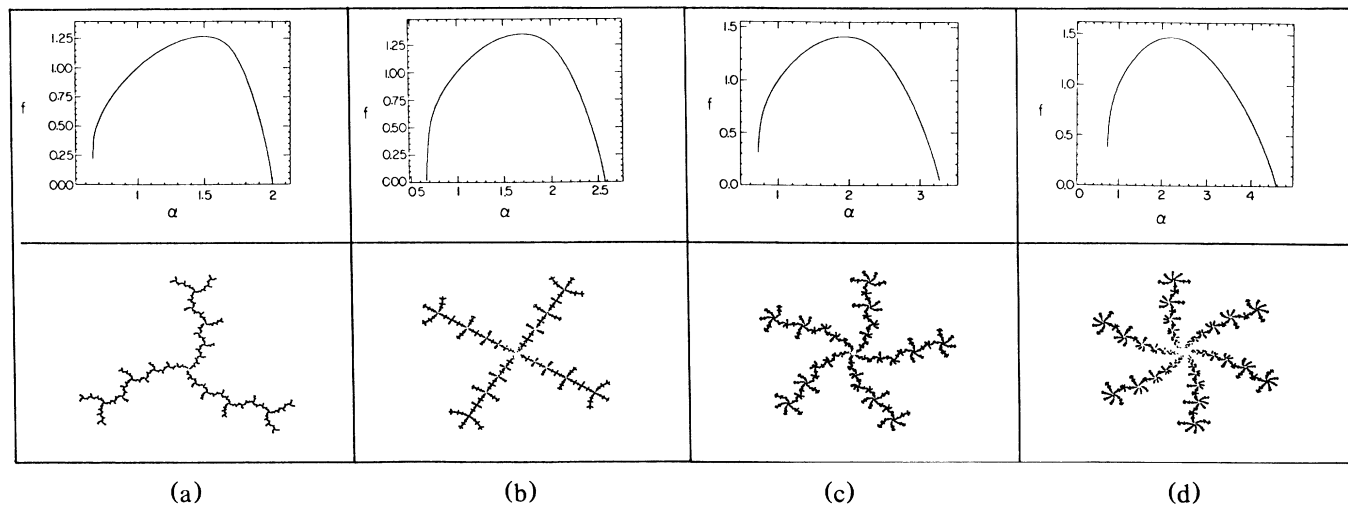


FIG. 1. Upper panel: Julia sets of the mappings $Z' = Z^m + C$ for $m=3-6$. The C values satisfy $(C^m + C)^m = C^m$. Lower panel: $f(\alpha)$ functions of the harmonic measure of the sets in the upper panel, respectively.

The models appear in the study of analytic maps of the complex plane to itself. Consider the mapping

$$Z' = Z^m + C, \tag{1}$$

where Z and C are complex. For almost all initial points in the complex plane, repeated iterations of (1) lead either to 0 or to ∞ . The set of points that remains invariant under (1) is the so-called Julia set.¹¹ The Julia set can be easily obtained by our solving either for the (unstable) periodic orbits of (1) or for one of the fixed points $Z^* = Z^{*m} + C$, and finding the preimages $(Z^* - C)^{1/m}$ (there are m of them). Each preimage gives rise to m further preimages, etc.

Julia sets come in a myriad of shapes,¹² most of them irrelevant to us. We are interested in dendritic (and connected) sets. These can be easily found by our choosing C such that $Z=0$ iterates to an unstable periodic orbit. (Such values of the parameter are called Misiurewicz points.) Examples of such Julia sets for $m=3, 4, 5$, and 6 are shown in Fig. 1. The gross features of the shapes are determined by m in $Z^m + C$, i.e., they have m main branches.

The relevance of these shapes to growth patterns is not

$$Z(\epsilon_n, \epsilon_{n-1}, \dots, \epsilon_1) - C = R(\epsilon_n, \epsilon_{n-1}, \dots, \epsilon_1) \exp[i\theta(\epsilon_n, \dots, \epsilon_1)],$$

the recursive encoding is obtained from

$$Z(\epsilon_{n+1}, \epsilon_n, \dots, \epsilon_1) = F_{\epsilon_{n+1}}(Z(\epsilon_n, \dots, \epsilon_1)) = [R(\epsilon_n, \dots, \epsilon_1)]^{1/m} \exp\{i[\theta(\epsilon_n, \dots, \epsilon_1) + 2\pi\epsilon_{n+1}/m]\}. \tag{2}$$

The encoding at the n th generation can be written also as $Z(t)$, with $t = \sum_{j=0}^n \epsilon_j m^{-j}$. We can cover the set in the n th generation with balls of diameter

$$l(\epsilon_n, \epsilon_{n-1}, \dots, \epsilon_1) = |Z(t + m^{-n}) - Z(t)|.$$

Denoting as usual¹⁸ the generalized dimensions of this set by D_q and $\tau(q) \equiv (q-1)D_q$, we solve for $q(\tau)$ from

$$m^{q(\tau)} = \sum_{\epsilon_1, \dots, \epsilon_n} |l(\epsilon_n, \dots, \epsilon_1)|^{-\tau}. \tag{3}$$

just in their appearance. The deep statement is that, in fact, by our starting a construction of the set from any of its points (say one of the fixed points) and iterating backwards $(Z - C)^{1/m}$, choosing randomly one of the m preimages at each step, the distribution of points obtained naturally is a harmonic measure.¹³⁻¹⁵ In other words, the rate of visitation of a little ball containing a piece of the set by the iterates is the same as the probability that a random walker launched at infinity would hit that ball. The advantage here, however, is that we can properly encode the set via symbolic dynamics^{16,17} and therefore calculate all the scaling properties systematically.

The symbolic encoding is done as follows: Write the fixed points of $Z^m + C$ as $Z^* = |Z^*| \exp(i\phi^*)$. The fixed point with the smallest positive ϕ^* is denoted in the first generation by $Z(0)$. Set now $Z^* - C = R^* \exp(i\theta^*)$. The preimages of the fixed point are denoted by

$$Z(\epsilon_1, 0) = R^{*1/m} \exp\{i[\theta^* + 2\pi\epsilon_1/m]\},$$

where ϵ_1 takes on m values $0, 1, 2, \dots, m-1$. If we then write

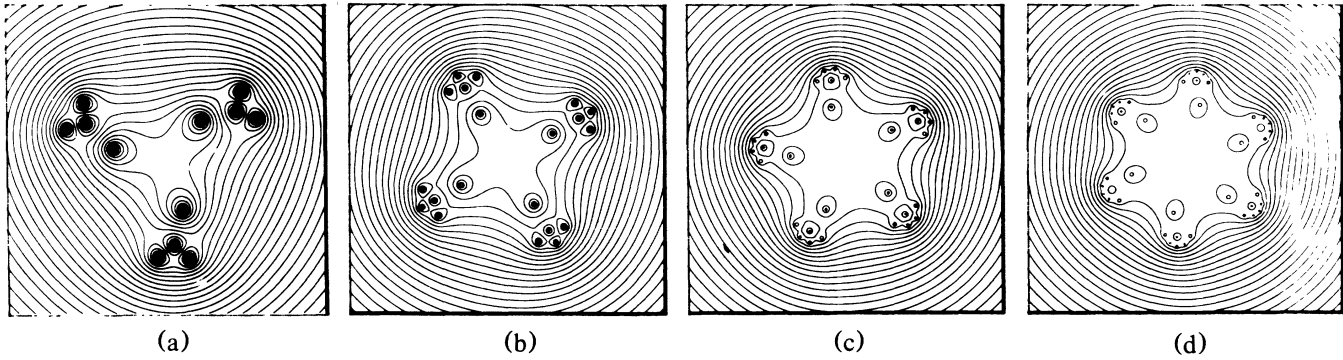


FIG. 2. Equipotential contours for the electrically charged sets of Fig. 1.

Notice that we have explicitly used the fact that all preimages are taken equiprobable,¹⁹ to turn the usual⁷ partition function equation $\sum P_i^q/l_i^r = 1$ into (3).

To solve for $q(\tau)$ we use a powerful tool that was recently developed,¹⁹ which yields $m^{q(\tau)}$ as the largest eigenvalue $\lambda(\tau)$ of an eigenvalue equation $\lambda\psi = L\psi$. The derivation, theory, and methods of solution of such eigenvalue equations are available in great detail elsewhere,²⁰ and here we shall simply state the equation and display its solutions.

With use of the functions $F_\epsilon(x)$ of Eq. (2), the relevant eigenvalue equation reads

$$\lambda(\tau)\psi^{(\tau)}(x) = \sum_\epsilon |F'_\epsilon(x)|^{-\tau} \psi^{(\tau)}(F_\epsilon(x)). \quad (4)$$

The function $q(\tau)$ of Eq. (3) is obtained from $q(\tau) = \log \lambda(\tau) / \log m$. Such an equation can be solved, for example, if we start with a constant function $\psi(x)$ and iterate Eq. (4), adjusting $\lambda(\tau)$ to the unique value that allows convergence. In all cases considered here, the second eigenvalue of L is significantly smaller than $\lambda(\tau)$, and therefore convergence is achieved very rapidly. Finally, the function $f(\alpha)$ is found as usual⁷ from the Legendre transform $\alpha = \partial \tau(q) / \partial q$, $f(\alpha) = q\alpha - \tau(q)$. The resulting $f(\alpha)$ curves for the Julia sets of $Z^m + C$, $m = 3-6$, are shown in Fig. 1. We believe that they are very well converged.

Consider first the values of α_{\min} for $m = 4-6$. These turn out to be 0.66, 0.71, and 0.75, respectively. Evidently, these values agree very well with the expectation of a large-wedge model, in which $\alpha_{\min} = m/(m+2)$. To understand the applicability of a large-wedge model we draw now the equipotential lines for our ramified fractals. In this case we can obtain a closed-form formula for the potential. This can be done since there exists for any map $Z' = g_c(Z) = Z^m + C$ a conformal mapping h_c such that $h_c \circ g_c \circ h_c^{-1} = g_0$. For g_0 (i.e., $Z' = Z^m$), the Julia set is the circle, with the potential $\phi_0 = \ln|x|$. The potential ϕ_c of the Julia set of $g_c(Z)$ is $\ln|h_c(x)|$. After some manipulations one can derive¹¹ the exact formula

for the potential ϕ_c :

$$\phi_c(x) = \ln|x| + \sum_{n=1}^{\infty} \frac{1}{m^n} \ln \left| 1 + \frac{C}{[g_c^{n-1}(x)]^m} \right|. \quad (5)$$

Figure 2 displays equipotential contours for the sets whose $f(\alpha)$ curves are shown in Fig. 1. It is immediately apparent why the large-wedge model works so well for $m = 4, 5, 6$. The symmetries of the fractals are reflected in the contour lines right up to the very tips of the set and, in fact, are quite the same as potential lines of squares, pentagons, and hexagons, respectively. One should stress that the large-wedge model is not guaranteed to work. For example, for $m = 3$ it predicts $\alpha_{\min} = \frac{3}{5}$. In fact, the α_{\min} of the set in Fig. 1(a) is $\alpha \approx 0.66$. The bifurcated nature of the branches cause the potential lines to curve into right angles locally near the major tips [see Figs. 1(a) and 2(a)]. The large-wedge model is expected to work only when the major branches carry subbranches that do not extend far enough to perturb the contours of the equipotential lines.

To understand the value of α_{\max} , focus on C values such that $Z = 0 \rightarrow C \rightarrow Z^*$, where Z^* is a fixed point. (Other Misiurewicz points conform to similar considerations.) We expect α_{\max} to be the scaling near $Z = 0$, which is at the root of the branches: The only way for the iteration to fall near $Z = 0$ is for it to fall near C , whose preimage is $Z = 0$. The probability to fall within a distance δ_n of C , after n random iterations, scales with n like the probability to fall within a distance δ_n of the fixed point Z^* . However, this is the probability to see an itinerary ϵ^n , which is precisely $(1/m)^n$. The size of δ_n scales like $\delta_n = [m|Z^*|^{m-1}]^{-n}$. With use of $p(l) \sim l^\alpha$, this estimate yields immediately the scaling exponent in the vicinity of the fixed point, α^* , as $\alpha^{*-1} = 1 + (m-1) \log(Z^*) / \log m$. (Notice that if this fixed point falls at the tip of a branch, as it often does, this will be also α_{\min} , and indeed this estimate is found in such cases to be excellent.) Once we fall at a distance δ_n from C , say to $Z = C + \delta_n$, the distance to zero in the next iteration is

$\xi_n = (C + \delta_n - C)^{1/m} = \delta_n^{1/m}$. Since the probability to get there still scales like $(1/m)^n$, we conclude that $\alpha_{\max} = m\alpha^*$. If $\alpha^* = \alpha_{\min}$, then $\alpha_{\max} = m\alpha_{\min}$. If not, we can state that $\alpha_{\max} \geq m\alpha_{\min}$. This conclusion is borne out by the numerical results; see Fig. 1.

We thus find that for the family of models at hand, both α_{\min} and α_{\max} can be estimated directly from the geometry. The narrower the fjords are, the stronger is the exponential falloff of the harmonic measure in them. In the case of m branches where the large-wedge model works, $\alpha_{\min} = m/(m+2)$ and $\alpha_{\max} \geq m^2/(m+2)$.

Evidently, if the large-wedge model works for the (rather skinny) sets of Fig. 2, it is no less reasonable for the (more bushy) DLA. We thus feel that Ball's argument should be taken seriously. However, the major consequence of this Letter, in our opinion, is that there is good reason to believe that there exists an analytic representation of DLA in terms of Julia sets of appropriate polynomial or rational functions of the complex plane, such that $f(\alpha)$ of the harmonic measure balances the above mentioned instabilities. A stationary $f(\alpha)$ is expected to conform with $D_0 = 1 + \alpha_{\min}$, and α_{\max} considerably larger than $m\alpha_{\min}$ (a "phase transition" with $\alpha_{\max} \rightarrow \infty$ cannot be excluded²¹). We are currently making an attempt to find such an analytical description that, if successful, would be reported elsewhere.

This work has been supported in part by the U.S.-Israel Binational Science Foundation and the Minerva Foundation (Munich, Germany). Stimulating bitnet discussions with Mogens Jensen, who independently thought of using Julia sets as probes of growth patterns, are gratefully acknowledged.

¹Y. Sawada, A. Dougherty, and J. P. Gollub, Phys. Rev. Lett. **56**, 1260 (1986).

²D. A. Weitz and M. Oliveria, Phys. Rev. Lett. **52**, 1433 (1984).

³L. Niemeyer, L. Pietronero, and H. J. Weismann, Phys. Rev. Lett. **52**, 1033 (1984).

⁴R. Lenormand, Physica (Amsterdam) **140A**, 114 (1986); J. Nittmann, G. Daccord, and H. E. Stanley, Nature (London) **314**, 141 (1985); E. Ben-Jacob, R. Godbey, N. D. Goldenfeld, J. Koplik, H. Levine, T. Mueller, and L. M. Sander, Phys. Rev. Lett. **55**, 1315 (1985).

⁵T. A. Witten and L. M. Sander, Phys. Rev. Lett. **47**, 1400 (1981).

⁶T. C. Halsey, P. Meakin, and I. Procaccia, Phys. Rev. Lett. **56**, 854 (1986).

⁷T. C. Halsey, M. H. Jensen, L. P. Kadanoff, I. Procaccia, and B. I. Shraiman, Phys. Rev. A **33**, 1141 (1986).

⁸L. P. Turkevich and H. Scher, Phys. Rev. Lett. **55**, 1026 (1985).

⁹See J. S. Langer, Rev. Mod. Phys. **52**, 1 (1980).

¹⁰R. C. Ball, Physica (Amsterdam) **140A**, 62 (1986).

¹¹M. J. Feigenbaum, I. Procaccia, and T. Tel, to be published.

¹²For an introduction, see R. Devaney, *An Introduction to Chaotic Dynamical Systems* (Benjamin, Menlo Park, 1986).

¹³H.-O. Peitgen and P. H. Richter, *The Beauty of Fractals* (Springer-Verlag, Berlin, 1986).

¹⁴A. Manning, "The Dimension of the Maximal Measure for a Polynomial Map" (unpublished).

¹⁵N. G. Makarou, Proc. London Math. Soc. **51**, 369 (1985).

¹⁶L. Carleson, "On the Support of Harmonic Measure for Sets of Cantor Type" (to be published).

¹⁷P. Collet and J.-P. Eckmann, *Iterated Maps of the Interval as Dynamical Systems* (Birkhauser, Boston, 1980).

¹⁸M. H. Jensen, L. P. Kadanoff, and I. Procaccia, Phys. Rev. A **36**, 1409 (1987).

¹⁹H. G. E. Hentschel and I. Procaccia, Physica (Amsterdam) **8D**, 435 (1983).

²⁰M. J. Feigenbaum, M. H. Jensen, and I. Procaccia, Phys. Rev. Lett. **57**, 1503 (1986).

²¹M. H. Jensen, private communication.